Hindawi Publishing Corporation
International Journal of Photoenergy
Volume 2015, Article ID 790242, 7 pages
http://dx.doi.org/10.1155/2015/790242

Research Article

Influence of Substrate on Crystal Orientation of Large-Grained Si Thin Films Formed by Metal-Induced Crystallization

Kaoru Toko,[1] Mitsuki Nakata,[1] Atsushi Okada,[1] Masato Sasase,[2] Noritaka Usami,[3,4] and Takashi Suemasu[1,4]

[1] *Institute of Applied Physics, University of Tsukuba, Tsukuba, Ibaraki 305-8573, Japan*
[2] *The Wakasa Wan Energy Research Center, Tsuruga, Fukui 914-0192, Japan*
[3] *Materials, Physics and Energy Engineering, Nagoya University, Aichi 464-8603, Japan*
[4] *Japan Science and Technology Agency, CREST, 5 Sanbancho, Chiyoda-ku, Tokyo 102-0075, Japan*

Correspondence should be addressed to Kaoru Toko; toko@bk.tsukuba.ac.jp

Received 17 July 2014; Revised 18 December 2014; Accepted 8 January 2015

Academic Editor: Serap Gunes

Producing large-grained polycrystalline Si (poly-Si) film on glass substrates coated with conducting layers is essential for fabricating Si thin-film solar cells with high efficiency and low cost. We investigated how the choice of conducting underlayer affected the poly-Si layer formed on it by low-temperature (500°C) Al-induced crystallization (AIC). The crystal orientation of the resulting poly-Si layer strongly depended on the underlayer material: (100) was preferred for Al-doped-ZnO (AZO) and indium-tin-oxide (ITO); (111) was preferred for TiN. This result suggests Si heterogeneously nucleated on the underlayer. The average grain size of the poly-Si layer reached nearly 20 μm for the AZO and ITO samples and no less than 60 μm for the TiN sample. Thus, properly electing the underlayer material is essential in AIC and allows large-grained Si films to be formed at low temperatures with a set crystal orientation. These highly oriented Si layers with large grains appear promising for use as seed layers for Si light-absorption layers as well as for advanced functional materials.

1. Introduction

High-quality crystalline Si on glass has been widely studied for use in low-cost thin-film solar cells with high-conversion efficiencies [1, 2]. In a polycrystalline Si (poly-Si) thin film, if its grain size is sufficiently larger than the cell thickness (~10 μm), the poly-Si cell can approach the efficiency of single-crystal Si wafer [2, 3]. Additionally, controlling the crystal orientation of the poly-Si film is essential for forming an effective antireflection structure [4] as well as for producing epitaxial seeds, used as starting materials for advanced functional materials [5] or aligned nanowires [6].

To form polycrystalline semiconductors on glass, aluminum-induced crystallization (AIC) is a possible technique that has received much attention [7, 8]. In this technique, an amorphous Si (a-Si) layer on an Al layer is transformed into a crystalline phase via exchange between the Al and Si layers during annealing at low temperatures (425–500°C) [9–11]. Additionally, AIC can grow either (100)- or (111)-oriented poly-Si films with large grains (diameters of 10–100 μm) by controlling the initial Al thickness [11], the interface between the Al and Si [12], and the growth temperature [13, 14]. AIC-Si is being researched as a seed layer for homoepitaxial growth of a Si light-absorption layer to obtain high-efficiency thin-film solar cells [2, 15, 16].

To measure its photovoltaic properties, AIC-Si on a glass substrate coated with a conducting layer should be developed [17]. There are two approaches: inverted AIC [14, 18] and AIC on conducting layers [19]. Both techniques produced poly-Si with large grains (10–50 μm) on conducting layers. However, it is still uncertain how the conducting layer affects the crystal quality of AIC-Si. Recently we found that the crystal quality of AIC-Ge depends on the materials contacting Ge [20, 21]. In the present study, we prepared various conducting layers

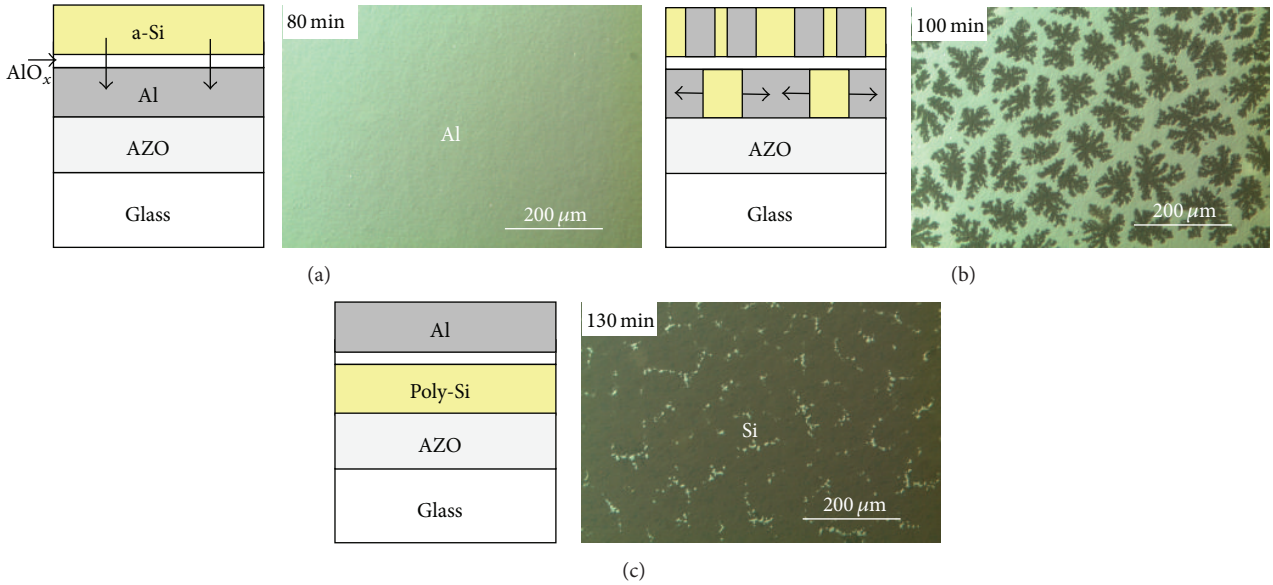

Figure 1: Schematic cross-sections and optical micrographs for a sample with an AZO underlayer, annealed at 500°C for (a) 80 min, (b) 100 min, and (c) 130 min. Each diagram corresponds to its respective optical micrograph showing the back surface of the sample through the transparent AZO and glass.

on glass, grew AIC-Si layers on them, and investigated the crystal quality of those AIC-Si layers. We found that the underlayer significantly influences the crystal orientation and grain size of the poly-Si films, demonstrating the importance of selecting a proper conducting layer.

2. Experiment

The thin films were prepared using radio-frequency (RF) magnetron sputtering (Sanyu Electron SVC-700RF) with an Ar sputtering pressure of 0.2 Pa and RF power of 100 W. Al-doped-zinc-oxide (AZO, Al_2O_3: 2%), indium-tin-oxide (ITO, SnO_2: 10%), and titanium nitride (TiN) layers, each 300 nm thick, were prepared on 1×1 cm SiO_2 0.6 mm-thick glass substrates (Furuuchi Chemical Corporation). The deposition rate was 24 nm min^{-1} for AZO, 28 nm min^{-1} for ITO, and 3.8 nm min^{-1} for TiN. Before deposition, the substrates were cleaned with acetone, methanol, and distilled water sequentially. For comparison, we also deposited on a bare SiO_2 substrate. During deposition, the substrate temperature was kept at 300°C for AZO and ITO and at room temperature (RT) for TiN. After depositing the underlayers, 100 nm-thick Al and 100 nm-thick Si layers were prepared at RT, with a deposition rate of 15 nm min^{-1} for Si and 23 nm min^{-1} for Al. Between the Al and Si deposition cycles, the Al layers were exposed to air for 48 h to form native AlO_x membranes, limiting the diffusion of Si and Al. Finally, the samples were annealed in N_2 at 500°C for 5 h to induce layer exchange between the Al and Si layers.

3. Results

Figures 1(a)–1(c) show the expected schematics of the crystallization stages for the sample with an AZO underlayer, with corresponding micrographs. The micrographs suggest that Si atoms diffuse into the Al layer, grow laterally, and cover the entire region during annealing. The detailed mechanism of this layer exchange has been well investigated in previous studies on AIC [9–11]. We found similar growth morphologies for the samples with the ITO, TiN, and SiO_2 underlayers.

The cross-sectional structure of the sample with the AZO underlayer was evaluated using transmission electron microscopy (TEM) and energy dispersive X-ray spectroscopy (EDX). Figures 2(a) and 2(c) show low-magnification TEM images before and after annealing, respectively, revealing uniform laminate structures. Figures 2(b) and 2(d) show EDX maps obtained at the same locations as in Figures 2(a) and 2(c), respectively. These EDX maps show that the layer exchange between the Al and Si layers occurred during annealing, causing Si to stack on AZO. The AlO_x membrane between the Si and Al layers was not clearly detected because it is thin (~1 nm) [7, 12]. The magnified TEM image in Figure 2(e) shows no dislocations or stacking faults in the Si layer, so the AIC technique can be used to form a high-quality Si layer on a conducting layer as well as on a bare glass substrate [11, 13].

After removing the aluminum and oxide layers, the crystal orientations of the poly-Si layers were characterized using electron backscatter diffraction (EBSD). Prior to this, the aluminum and oxide layers on the poly-Si layers were etched using an HF solution (HF: 1.5%) for 1 min. Figures 3(a)–3(d) show EBSD images in the normal direction (ND) for poly-Si layers on SiO_2, AZO, ITO, and TiN underlayers. The crystal orientation in the ND strongly depended on the underlayer material: Figures 3(a) and 3(d) indicate preferential (111) orientation for the SiO_2 and TiN samples, while Figures 3(b) and 3(c) indicate preferential (100) orientation for the AZO and ITO samples. Figures 3(e)–3(h) show EBSD images in the

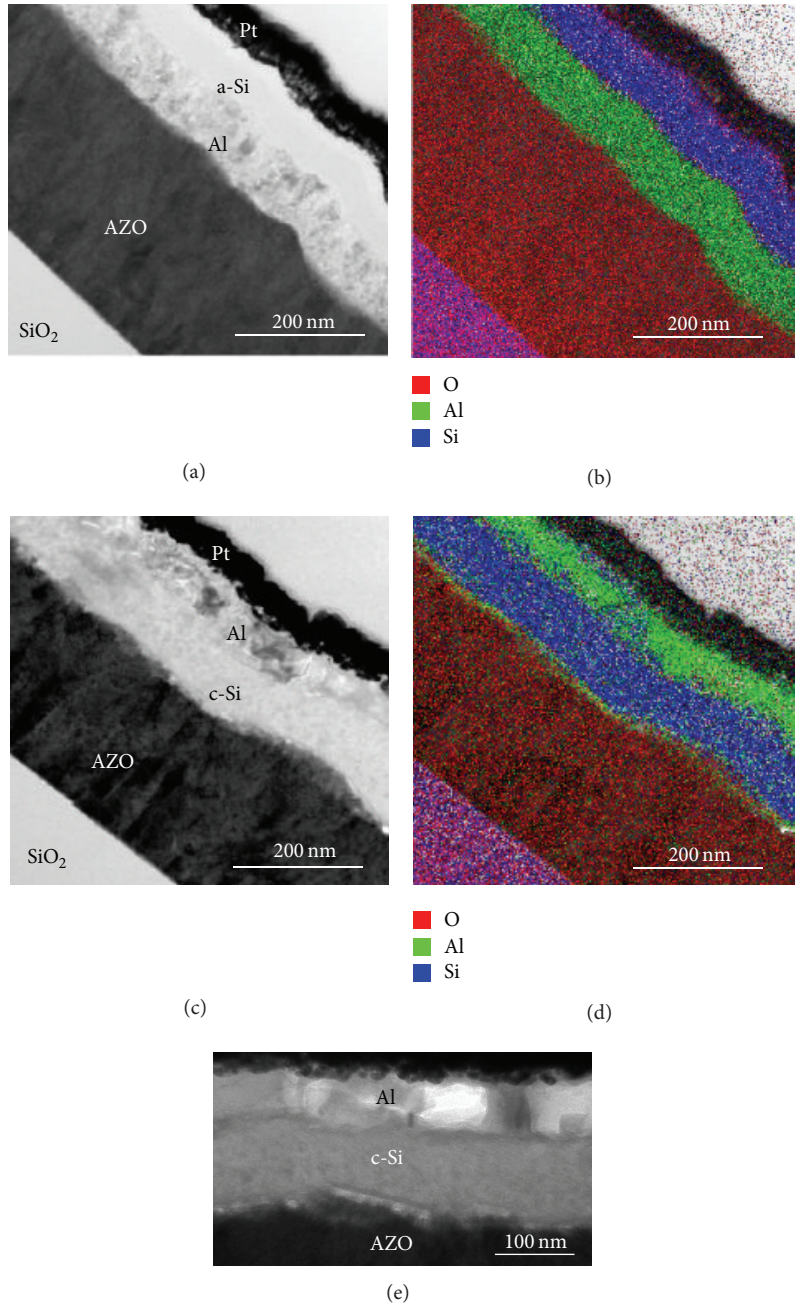

Figure 2: Cross-sectional TEM images and EDX maps for a sample with an AZO underlayer: (a, b) before and (c, d) after annealing (500°C, 5 h), indicating that layer exchange occurred. (e) Magnified TEM image of the sample after annealing.

transverse direction (TD) obtained at the same locations as in Figures 3(a)–3(d), respectively. The black solid lines indicate random grain boundaries, drawn based on EBSD analysis. All the samples had large grains with diameters of more than 10 μm.

Figures 4(a)–4(d) show the area fractions of the crystal orientation in the poly-Si layers as functions of angles from ⟨100⟩ and ⟨111⟩ directions. The total preferential orientation fractions, defined as the integrated values of area fractions from 0° to 20°, were calculated as follows: 99% (111) for the SiO_2 sample, 94% (100) for the AZO sample, 88% (100) for the ITO sample, and 93% (111) for the TiN sample. Figures 4(e)–4(h) show the area-fraction distributions of the grain diameters in the AIC-Si layers. The average grain diameters were calculated as follows: 105 μm for the SiO_2 sample, 19 μm for the AZO sample, 18 μm for the ITO sample, and 68 μm for the TiN sample. The grain sizes of AIC-Si were smaller on the conducting layers than on SiO_2; however, all these grain sizes are one order of magnitude larger than those of the poly-Si layers formed by conventional solid-phase crystallization

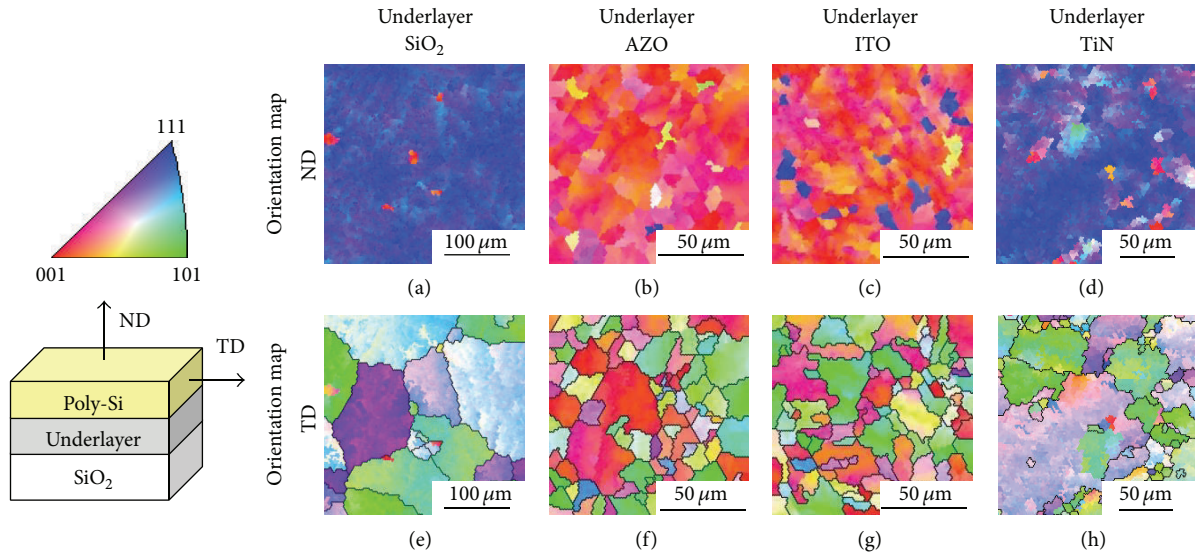

FIGURE 3: EBSD images of the poly-Si layers with SiO_2, AZO, ITO, and TiN underlayers. (a)–(d) ND and (e)–(h) TD relative to the substrate; the ND and TD maps are of the same regions for each sample. The colors indicate the crystal orientation, according to the inserted color key. The black solid lines in the TD maps indicate random grain boundaries.

[17, 22]. In particular, the poly-Si we produced on TiN had the largest grain size among AIC-Si on conducting layers [18, 19]. These results indicate that selecting a proper conducting layer is essential to AIC for obtaining high-quality Si layers.

4. Discussion

Here, we will discuss how the crystal orientation depended on the underlayer. The surface roughness of the conducting underlayers was measured using atomic force microscopy (AFM). The root-mean-square (RMS) roughness was 0.5 nm for SiO_2, 11.6 nm for AZO, 4.9 nm for ITO, and 5.5 nm for TiN. The EBSD results show no clear correlation between the underlayer roughness and the crystal orientation of the AIC-Si layers. Because the substrate influences the crystal quality of a solid-phase-crystallized semiconducting film when its nucleation occurs at the substrate [23], we attribute the dependence of the crystal orientation on the underlayer as a consequence of the interfacial energy between Si and the underlayer material.

Figure 5 shows a schematic cross-section of a sample with the vertical distribution of Si concentration. In AIC, Si atoms diffuse into the Al layer from the a-Si layer through the AlO_x membrane [11, 12, 24]. Because the Si diffusion rate in Al (1.7×10^{-7} cm^2 s^{-1}) is several orders of magnitude higher than that in AlO_x (3.5×10^{-15} cm^2 s^{-1}) while, annealing at 500°C, the Si concentration in Al, C_{Al} is constant throughout the Al layer [11]. In this case, Si can nucleate heterogeneously at the surface of the underlayer. Experimental results in our previous reports on thickness-dependent AIC of Si [14] and Ge [20] also suggest that this nucleation heterogeneously occurs at the surface of the substrate (SiO_2) when the Al layer is thin (≤100 nm) and that a preferential (111) orientation is caused by minimization of interfacial energy between Si(Ge) and SiO_2. Thus, we conclude that Si nucleation likely occurs at the underlayer. Though it is difficult to obtain the true interfacial energies between Si and underlayers consisting of compound materials, the difference of interfacial energy is a possible reason behind the varying crystal orientation of AIC-Si.

5. Conclusion

We investigated how underlayers affected the crystal quality of AIC-Si in order to obtain high-quality poly-Si on a conducting-layer-coated glass substrate. AIC allowed for low-temperature (500°C) formation of large-grained poly-Si films on conducting layers (AZO, ITO, and TiN). The crystal quality of the poly-Si varied dramatically on different underlayers: the grain size and crystal orientation fraction of the resulting poly-Si layers were 105 μm and 99% (111) for the SiO_2 sample, 19 μm and 94% (100) for the AZO sample, 18 μm and 88% (100) for the ITO sample, and 68 μm and 93% (111) for the TiN sample. These results suggest that the Si nucleated heterogeneously on the underlayer. The poly-Si we produced on TiN had the largest grain size among all reports of poly-Si on conducting layers so far. Thus, we conclude that selecting a proper underlayer is absolutely essential to AIC and that AIC is effective for obtaining large-grained Si films with a set crystal orientation. This finding will be useful for fabricating poly-Si thin-film solar cells, allowing for high performance at low cost.

Conflict of Interests

The authors declare that there is no conflict of interests regarding the publication of this paper.

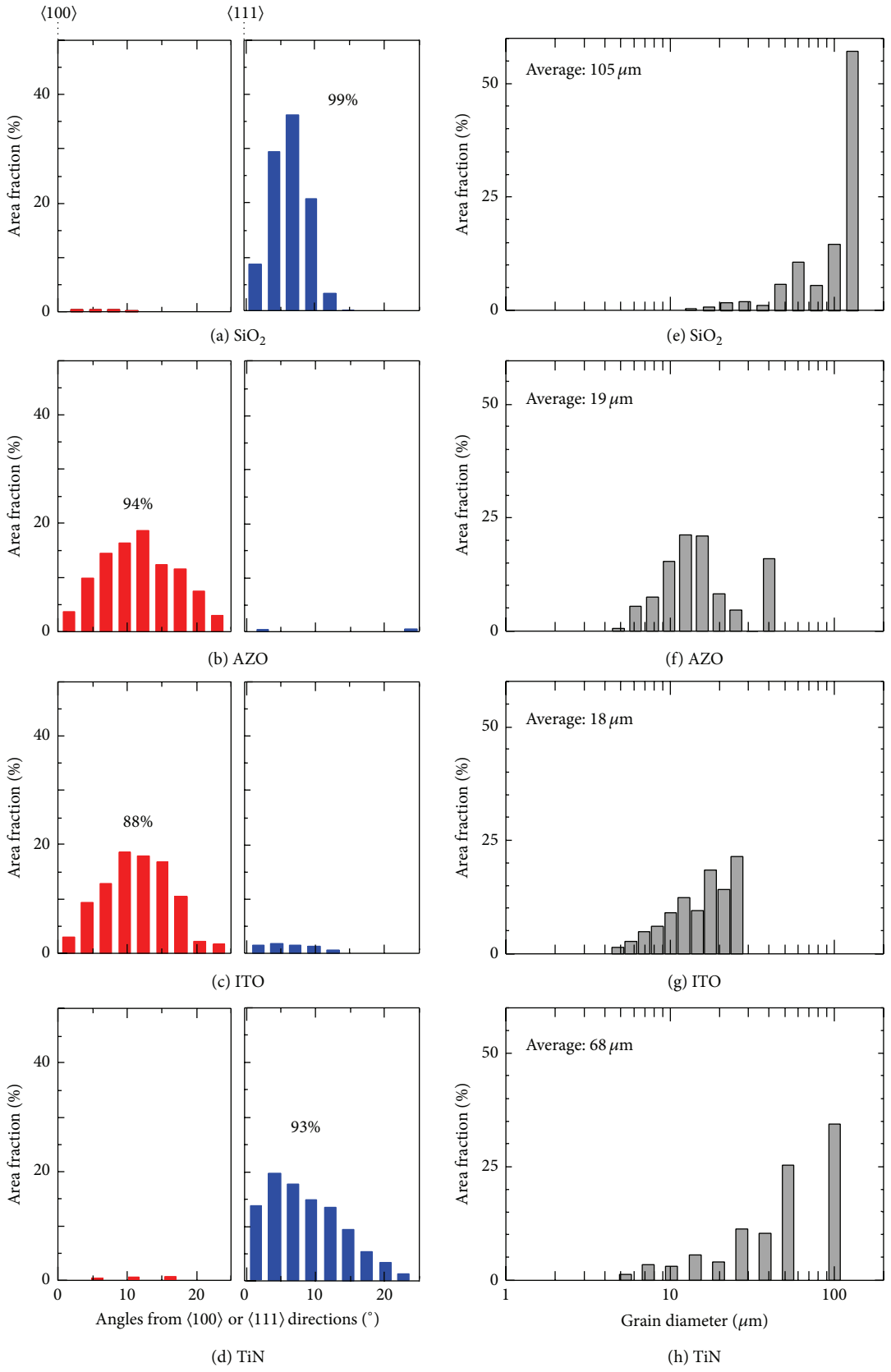

FIGURE 4: Distribution histograms of the (a)–(d) crystal orientation fraction and the (e)–(h) grain size in the poly-Si layers with SiO_2, AZO, ITO, and TiN underlayers. These histograms were obtained from the orientation maps shown in Figure 3. The integrated values of the preferentially oriented area fraction from 0° to 20° are shown in (a)–(d); the average grain sizes are shown in (e)–(h).

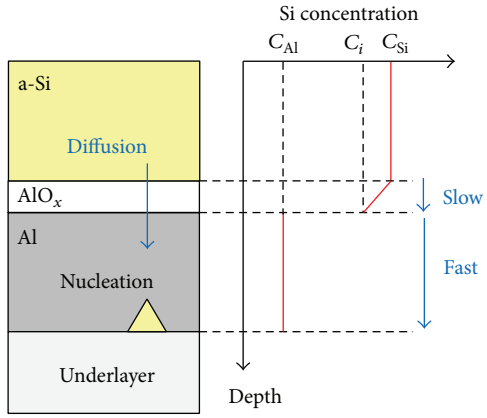

FIGURE 5: Schematic of Si heterogeneous nucleation during AIC with a vertical distribution of Si concentration in the sample. C_{Si} is the atomic concentration in the a-Si layer, C_i is the Si concentration at the bottom of the AlO_x membrane, and C_{Al} is the Si concentration in the Al layer. The crystal orientation of nuclei is determined by the interfacial energy between Si and the underlayer.

Acknowledgments

This work was financially supported by the Japan Science and Technology Agency, CREST, the Yazaki Memorial Foundation for Science and Technology, and the Asahi Glass Foundation.

References

[1] M. A. Green, "Crystalline and thin-film silicon solar cells: state of the art and future potential," *Solar Energy*, vol. 74, no. 3, pp. 181–192, 2003.

[2] W. Fuhs, S. Gall, B. Rau, M. Schmidt, and J. Schneider, "A novel route to a polycrystalline silicon thin-film solar cell," *Solar Energy*, vol. 77, no. 6, pp. 961–968, 2004.

[3] M. Imaizumi, T. Ito, M. Yamaguchi, and K. Kaneko, "Effect of grain size and dislocation density on the performance of thin film polycrystalline silicon solar cells," *Journal of Applied Physics*, vol. 81, no. 11, pp. 7635–7640, 1997.

[4] P. Campbell, S. R. Wenham, and M. A. Green, "Light trapping and reflection control in solar cells using tilted crystallographic surface textures," *Solar Energy Materials and Solar Cells*, vol. 31, no. 2, pp. 133–153, 1993.

[5] D. Tsukada, Y. Matsumoto, R. Sasaki et al., "Photoresponse properties of polycrystalline $BaSi_2$ films grown on SiO_2 substrates using (111)-oriented Si layers by an aluminum-induced crystallization method," *Applied Physics Express*, vol. 2, no. 5, Article ID 051601, 2009.

[6] Y. Cohin, O. Mauguin, L. Largeau et al., "Growth of vertical GaAs nanowires on an amorphous substrate via a fiber-textured Si platform," *Nano Letters*, vol. 13, no. 6, pp. 2743–2747, 2013.

[7] O. Nast and A. J. Hartmann, "Influence of interface and Al structure on layer exchange during aluminum-induced crystallization of amorphous silicon," *Journal of Applied Physics*, vol. 88, no. 2, pp. 716–724, 2000.

[8] K. Toko, M. Kurosawa, N. Saitoh et al., "Highly (111)-oriented Ge thin films on insulators formed by Al-induced crystallization," *Applied Physics Letters*, vol. 101, no. 7, Article ID 072106, 2012.

[9] Y. Sugimoto, N. Takata, T. Hirota, K.-I. Ikeda, F. Yoshida, and H. Nakashima, "Low-temperature fabrication of polycrystalline Si thin film using Al-induced crystallization without native Al oxide at amorphous Si/Al interface," *Japanese Journal of Applied Physics*, vol. 44, no. 7, pp. 4770–4775, 2005.

[10] Z. Wang, L. Gu, L. P. H. Jeurgens, F. Phillipp, and E. J. Mittemeijer, "Real-time visualization of convective transportation of solid materials at nanoscale," *Nano Letters*, vol. 12, no. 12, pp. 6126–6132, 2012.

[11] A. Sarikov, J. Schneider, J. Berghold et al., "A kinetic simulation study of the mechanisms of aluminum induced layer exchange process," *Journal of Applied Physics*, vol. 107, no. 11, Article ID 114318, 2010.

[12] M. Kurosawa, N. Kawabata, T. Sadoh, and M. Miyao, "Orientation-controlled Si thin films on insulating substrates by Al-induced crystallization combined with interfacial-oxide layer modulation," *Applied Physics Letters*, vol. 95, no. 13, Article ID 132103, 2009.

[13] M. Jung, A. Okada, T. Saito, T. Suemasu, and N. Usami, "On the controlling mechanism of preferential orientation of polycrystalline-silicon thin films grown by aluminum-induced crystallization," *Applied Physics Express*, vol. 3, no. 9, Article ID 095803, 2010.

[14] K. Toko, R. Numata, N. Saitoh, N. Yoshizawa, N. Usami, and T. Suemasu, "Selective formation of large-grained, (100)- or (111)-oriented Si on glass by Al-induced layer exchange," *Journal of Applied Physics*, vol. 115, no. 9, Article ID 094301, 2014.

[15] I. Gordon, L. Carnel, D. Van Gestel, G. Beaucarne, and J. Poortmans, "Fabrication and characterization of highly efficient thin-film polycrystalline-silicon solar cells based on aluminium-induced crystallization," *Thin Solid Films*, vol. 516, no. 20, pp. 6984–6988, 2008.

[16] B.-R. Wu, S.-Y. Lo, D.-S. Wuu et al., "Direct growth of large grain polycrystalline silicon films on aluminum-induced crystallization seed layer using hot-wire chemical vapor deposition," *Thin Solid Films*, vol. 520, no. 18, pp. 5860–5866, 2012.

[17] C. Becker, E. Conrad, P. Dogan et al., "Solid-phase crystallization of amorphous silicon on ZnO:Al for thin-film solar cells," *Solar Energy Materials and Solar Cells*, vol. 93, no. 6-7, pp. 855–858, 2009.

[18] H. Kuraseko, N. Orita, H. Koaizawa, and M. Kondo, "Inverted aluminum-induced layer exchange method for thin film polycrystalline silicon solar cells on insulating substrates," *Applied Physics Express*, vol. 2, no. 1, Article ID 015501, 2009.

[19] K. Y. Lee, M. Muske, I. Gordon et al., "Large-grained poly-Si films on ZnO:Al coated glass substrates," *Thin Solid Films*, vol. 516, no. 20, pp. 6869–6872, 2008.

[20] K. Toko, K. Nakazawa, N. Saitoh, N. Yoshizawa, N. Usami, and T. Suemasu, "Orientation control of Ge thin films by underlayer-selected Al-induced crystallization," *CrystEngComm*, vol. 16, no. 13, pp. 2578–2583, 2014.

[21] K. Toko, R. Numata, N. Oya, N. Fukata, N. Usami, and T. Suemasu, "Low-temperature (180°C) formation of large-grained Ge (111) thin film on insulator using accelerated metal-induced crystallization," *Applied Physics Letters*, vol. 104, no. 2, Article ID 022106, 2014.

[22] K. Toko, M. Kurosawa, H. Yokoyama et al., "(100) orientation-controlled Ge giant-stripes on insulating substrates by rapid-melting growth combined with Si micro-seed technique," *Applied Physics Express*, vol. 3, no. 7, Article ID 075603, 2010.

[23] F. Edelman, Y. Komem, M. Bendayan, and R. Beserman, "Initial crystallization stage of amorphous germanium films," *Journal of Applied Physics*, vol. 72, no. 11, pp. 5153–5157, 1992.

[24] R. Numata, K. Toko, N. Saitoh, N. Yoshizawa, N. Usami, and T. Suemasu, "Orientation control of large-grained si films on insulators by thickness-modulated Al-induced crystallization," *Crystal Growth and Design*, vol. 13, no. 4, pp. 1767–1770, 2013.